Thermal cycling protects SH-SY5Y cells against hydrogen peroxide and β-amyloid-induced cell injury through stress response mechanisms involving Akt pathway

Wei-Ting Chen[1,2,¶], Yu-Yi Kuo[1,2,¶], Guan-Bo Lin[1,2,¶], Chueh-Hsuan Lu[1,2], Hao-Ping Hsu[3], Yi-Kun Sun[2], and Chih-Yu Chao[1,2,4,*]

[1] Department of Physics, Lab for Medical Physics & Biomedical Engineering, National Taiwan University, Taipei 10617, Taiwan

[2] Biomedical & Molecular Imaging Center, National Taiwan University College of Medicine, Taipei 10051, Taiwan

[3] Department of Medicine, National Taiwan University College of Medicine, Taipei 10051, Taiwan

[4] Graduate Institute of Applied Physics, Biophysics Division, National Taiwan University, Taipei 10617, Taiwan

* Corresponding author

E-mail: cychao@phys.ntu.edu.tw (CYC)

¶ These authors contributed equally to this work.

Abstract

Neurodegenerative diseases (NDDs) are becoming a major threat to public health, according to the World Health Organization (WHO). The most common form of NDDs is Alzheimer's disease (AD), boasting 60-70% share. Although some debates still exist, excessive aggregation of β-amyloid protein (Aβ) and neurofibrillary tangles has been deemed one of the major causes for the pathogenesis of AD. A growing number of evidences from studies, however, have suggested that reactive oxygen species (ROS) also play a key role in the onset and progression of AD. Although scientists have had some understanding of the pathogenesis of AD, the disease still cannot be cured, with existing treatment only capable of providing a temporary relief at best, partly due to the obstacle of blood-brain barrier (BBB). The study was aimed to ascertain the neuroprotective effect of thermal cycle hyperthermia (TC-HT) against hydrogen peroxide (H_2O_2) and Aβ-induced cytotoxicity in SH-SY5Y cells. Treating cells with this physical stimulation beforehand significantly improved the cell viability and decreased the ROS content. The underlying mechanisms may be due to the activation of Akt pathway and the downstream antioxidant and prosurvival proteins. The findings manifest significant potential of TC-HT in neuroprotection, via inhibition of oxidative stress and cell apoptosis. It is believed that coupled with the use of drugs or natural compounds, this methodology can be even more effective in

42 treating NDDs.

43

44 Introduction

45 According to the World Health Organization (WHO), the number of
46 dementia-induced deaths more than doubled between 2000 and 2016, making it the
47 5th leading cause for deaths worldwide in 2016, up from 14th place in 2000. Among
48 the various forms of dementia such as Alzheimer's disease (AD) and Parkinson's
49 disease (PD), AD is the most common one, accounting for 60–70% of the cases.
50 Typically, AD exhibits such features as deposition of cortical plaques caused by
51 excessive aggregation of β-amyloid protein (Aβ) and neurofibrillary tangles, and
52 progressive brain degeneration and deterioration of cognitive function among elderly
53 people. Although the exact mechanism of AD pathogenesis remains unknown, it is
54 believed that oxidative stress and activation of free radicals, induced by Aβ
55 aggregation, play a key role in AD pathogenesis [1].

56 Reactive oxygen species (ROS) are reactive chemical species containing oxygen,
57 which are generated as natural byproduct of oxygen metabolism. ROS play important
58 roles in cell signalling and homeostasis, and their concentrations in cells are subtlety
59 regulated by various antioxidant compounds and enzymes. However, with cells under
60 continuing environmental stress (e.g. ultraviolet, inflammatory cytokines, or

environmental toxins), the imbalance between prooxidants and antioxidants may cause chronic oxidative stress. Accumulation of ROS may cause cell death, accelerate cell ageing, or induce age-related diseases [2]. More and more research evidences have suggested that ROS plays a central role in the onset and progression of AD [3]. Therefore, the protection of neural cells against oxidative damage may be a potential strategy to treat AD. Several in vitro or in vivo studies have explored the function of antioxidant and antiapoptotic drugs in ameliorating AD [4-6] but the approach is time-consuming and costly, plus the safety concern, which limits the use of these drugs in AD treatment. Moreover, the blood-brain barrier (BBB) dampens the efficacy of these drugs, since over 98% of small molecule drugs and ~100% of large molecule drugs can not pass the BBB [7]. Therefore, a non-drug treatment may be more suited to AD patients.

Scientists have long been interested in the profound effects of heat on cells, and have utilized it in various types of thermotherapeutical applications such as physiotherapy, urology, and cardiology [8]. One promising and effective thermal therapy is the treatment of cancer by hyperthermia (HT) [9]. HT is used to kill cancer cells directly or to potentiate the cytotoxicity of radiation and certain chemotherapy drugs [10]. The ROS level increased by HT treatment has been identified to play an important role as an intracellular mediator of HT-induced cell death [11]. On the

contrary, it has also been reported that heat shock (HS) will induce many cellular defense, including the antioxidant effect. For example, Tchouagué *et al* demonstrated that HS-generated ROS is involved in induction of cellular defense molecules Prxs, GSH and G6PD through Nrf2 activation [12]. Mustafi *et al* also showed that heat stress upregulates the HSP70 and MnSOD levels through ROS and p38MAPK [13]. In addition to the thermal treatment, the beneficial effects of light treatment were also reported in literatures. The review article by Hamblin summarized some pre-clinical studies and clinical trials by light therapy for brain disorders [14]. The physical stimulation, therefore, holds great potential for AD or other neurodegenerative diseases (NDDs).

The study employed a special thermal therapy, applied at high and low temperatures alternately to achieve an effect similar to antioxidant and antiapoptotic drugs. In our previous study, we used this novel method, thermal cycle hyperthermia (TC-HT) for the treatment of pancreatic cancer, and found that this physical stimulation greatly improved the anticancer effect of propolis and polyphenols on PANC-1 cells without the heat-induced side effect [15, 16]. Traditional HS or HT employs continuous heating to achieve curative effect, but it is likely to cause neuron damage since damage to the central nervous system occurs within few minutes of exposure to 42°C [17]. Nevertheless, the feature of TC-HT is that it can avoid the

damage caused by HT, which is crucial for neuroprotection.

In this study, we applied the TC-HT strategy to human neural cell line SH-SY5Y, which has been extensively used in research on neurodegenerative damage in vitro, and examined the prosurvival effect of TC-HT on preventing oxidative damage induced by hydrogen peroxide (H_2O_2) and Aβ. The results showed that subjection of the cells to heat at high and low temperatures alternately beforehand ameliorated the H_2O_2 and Aβ-induced cytotoxicity in SH-SY5Y cells significantly. It was found that TC-HT not only performed superior protective effect than the traditional HS but also avoided thermal damage caused by continuous heating. Examination of the underlying mechanism also showed that TC-HT could activate specific neuroprotective proteins. These findings indicate that TC-HT is a promising thermal therapy, which sheds light on novel treatment for AD or other NDDs.

Materials and methods

Cell culture and treatment

The human neuroblastoma SH-SY5Y cells purchased from Bioresource Collection and Research Center (Hsinchu, Taiwan) were maintained in MEM/F-12 mixture containing 10% fetal bovine serum (HyClone; GE Healthcare Life Sciences) and 1% penicillin-streptomycin, supplemented with 1mM sodium pyruvate and 0.1 mM

non-essential amino acids. The cells were cultured at 37°C in a humidified incubator composed of 5% CO_2. SH-SY5Y cells were seeded in 96-well plates overnight. Cells were pretreated with HT or TC-HT by the Thermal Cycler (Applied Biosystems; Thermo Fisher Scientific, Inc.) relative to the control at room temperature (RT). After the treatment, the cells were maintained in a 37°C incubator for 4 h. Subsequently, the pretreated cells were induced to undergo apoptosis by adding H_2O_2 to the culture medium. Cell viability was measured 24 h after the H_2O_2 treatment. As for AD disease model, the cells were treated with 25 or 50 μM $A\beta_{25-35}$ protein solution. The Aβ stock solution was prepared by solubilizing the $A\beta_{25-35}$ peptide (Sigma-Aldrich; Merck KGaA) in sterile deionized water to a concentration of 1 mM and then incubated at 37°C for 3 days to allow self-aggregation before treatment. The TC-HT therapy was applied 4 h before the Aβ treatment for the pretreatment group and 1 h after Aβ treatment for the post-treatment group, and the cell viability was determined 4 days after the treatment. For the Akt inhibitor experiment, 12 or 25 μM LY294002 (Cell Signaling Technology, Inc.) was treated 1 h before the TC-HT.

Cell Viability Assay

The cell viability was determined by 3-(4,5-dimethylthiazol-2-yl)-2,5-diphenyltetrazolium bromide (MTT) (Sigma-Aldrich;

Merck KGaA) assay. In brief, the culture medium was replaced with MTT solution (0.5 mg/mL in MEM/F12) and incubated at 37°C for 4 h. Equal volume of the solubilizing buffer (0.01 M HCl and 10% SDS) was added to dissolve the formazan crystals. The 96-well plates were analyzed on a FLUOstar OPTIMA microplate reader (BMG Labtech, Ltd.) at 570 nm, and background absorbance at 690 nm was subtracted.

Lactate dehydrogenase (LDH) assay

The assay measures a stable enzyme LDH, which is released into the cell culture medium when cell membranes are damaged. LDH levels were measured using a Cytoscan LDH cytotoxicity assay kit (G-Biosciences; Geno Technology Inc.) according to the manufacturer's instructions. Briefly, the cells were seeded in 96-well plates and then incubated with H_2O_2 with or without thermal cycle pretreatment. For analysis, 50 µL culture mediums from all wells were transferred to a new 96-well plate, and 50 µL of reaction mixtures were added to each well and incubated at 37°C for 20 min. The absorbance was measured at 490 nm using a microplate reader (BMG Labtech, Ltd.).

ROS level detection

ROS levels of cells were detected using the fluorescent dye dihydroethidium (DHE) (Sigma-Aldrich; Merck KGaA). Cells pretreated with TC-HT or HT at 42.5°C high temperature setting for 8 cycles or 2 h, respectively, were challenged with H_2O_2. After the treatment of H_2O_2 for 24 h, cells were washed with PBS, and then incubated with 5 μM DHE dye for 20 min at 37°C in the dark. The fluorescence intensity emitted by DHE was measured by flow cytometry in the PE channel, and ROS levels were expressed as mean fluorescence intensity for comparison.

Mitochondrial membrane potential (MMP) measurement

The MMP was determined by flow cytometry using 3,3'-dihexyloxacarbocyanine iodide ($DiOC_6(3)$) (Enzo Life Sciences International Inc.). $DiOC_6(3)$ is a lipophilic cationic fluorescent dye which allows estimation of the percentage of cells with low MMP. Cells were pretreated with TC-HT or HT 4 h before the H_2O_2 treatment. After the treatment of H_2O_2 for 24 h, cells were harvested and suspended at a density of 1 x 10^6 cells/mL in 1 μM $DiOC_6(3)$ dye working solution. After incubation at 37°C for 15 min, $DiOC_6(3)$ intensity was analyzed by flow cytometry in the FITC channel.

Western blot analysis

The protein expression levels of SH-SY5Y cells were investigated by western blot

analysis. Cells treated with TC-HT, HT, or H_2O_2 were harvested and lysed in RIPA lysis butter (EMD Millipore). The cells were harvested within 24 h after H_2O_2 treatment, and the timing for different protein collections was adjusted based on previous literatures [18-20]. For HSP70 and HSP105, cells were lysed 16 h after H_2O_2 treatment. For p-Akt, Akt, Nrf2, CREB, IDE, PSMA3, and PSMC3, cells were lysed 15 h after H_2O_2 treatment. For HO-1, cells were lysed 18 h after H_2O_2 treatment. After centrifugation and supernatant collection, equal amounts of proteins were resolved by 10% SDS-PAGE and transferred to polyvinylidene fluoride membranes. After drying for 1 h at RT, the membranes were probed with p-Akt, Akt, Nrf2, p-CREB, PSMA3, PSMC3 (Cell Signaling Technology, Inc.), HO-1 (Enzo Life Sciences International Inc.), insulin-degrading enzyme (Abcam) and GAPDH (GeneTex, Inc.) antibodies overnight at 4˚C. The washed membranes were then incubated with horseradish peroxidase-conjugated goat anti-rabbit secondary antibodies (Jackson ImmunoResearch Laboratories, Inc.). Immunoreactivity was visualized with an enhanced chemiluminescence substrate (Advansta, Inc.) and detected with the Amersham Imager 600 imaging system (GE Healthcare Life Sciences). The images were analyzed with Image Lab software (Bio-Rad Laboratories, Inc.).

Statistical analysis

The results were presented as the mean ± standard deviation. Statistical analyses using one-way analysis of variance (ANOVA) followed by Tukey's post-hot test were performed by OriginPro 2015 software (OriginLab). P-value < 0.05 was considered to indicate a statistically significant difference.

Results

In vitro-applied TC-HT

We applied the thermal cycle (TC) treatment to SH-SY5Y cells by a modified polymerase chain reaction (PCR) equipment (Fig 1C). Briefly, in our design, some protruding parts of the PCR machine and plastic well were milled so that the bottom of the well can touch the heat sink tightly. The basic TC settings were schemed as Fig 1A, where the temperature was elevated to the desired high temperature and sustained for a period of time followed by a cooling process at body temperature. It's worth noting that the adjustment of TC parameters (temperature and time) is based on the needs and objectives of the experiments. In our experiments, the TC parameters were set to high temperatures of 42.5°C or 41.5°C for 15 min, then lowered to 37°C and lasted for 35 sec. This cycle was repeated 8 or 12 times. The HT group maintains the same high temperature setting throughout the treatment in a continuous manner

without a break. To determine the actual temperatures of the cells, a needle thermocouple located in the bottom of the well was used to monitor the temperatures. Fig 1B represents the actual temperature measured by the thermocouple every 20 sec. The actual cycle temperature sensed by the cells was ~42-40.3°C for the setting of 42.5-37°C and ~40.9-39.4°C for 41.5-37°C setting, as shown in Fig 1B.

Fig 1. The setup of TC-HT. (A) Schematic representation of TC parameter settings. (B) Measurement of the cell temperature during the TC treatment by the thermocouple. (C) Image of the TC controller setup.

Effect of TC-HT on H_2O_2 and Aβ-induced cytotoxicity in SH-SY5Y cells

We applied H_2O_2 to SH-SY5Y cells as an oxidative stress and the cell viability was assessed by MTT assay. As shown in Fig 2A, treatment of H_2O_2 on SH-SY5Y cells for 24 h induced significant decrease of cell viability in a dose-dependent manner. Treatment of SH-SY5Y cells with 450 μM H_2O_2 for 24 h reduced the cell viability to 52.9% compared to control cells, which was used in the following experiments. To investigate whether TC-HT or HT produced protection and increased cell survival against the oxidative stress induced by H_2O_2, the SH-SY5Y cells were pretreated with

TC-HT or HT in the experiments. Two high temperature parameters (41.5°C or 42.5°C) were applied for 2 h or 3 h continuously in the HT group, and 8 or 12 cycles (for 15 min heating time per cycle) in the TC group to make the total thermal doses of the HT and TC groups equal. After the heat pretreatment, the treated SH-SY5Y cells were kept in the incubator at 37°C for 4 h. They were then challenged with H_2O_2 to generate the oxidative stress, and the cell viability was determined by MTT assay at 24 h after the H_2O_2 treatment. The results found that H_2O_2 treatment significantly reduced the viability of SH-SY5Y cells to 53.7% of the control value, and showed that the heat pretreatment conferred protective effect and increased the cell viability. At 41.5°C for 2 h and 8 cycles, HT and TC treatments increased the cell viability to 61.9% and 68.5% of the control value, respectively (Fig 2B). As we increased the high temperature setting to 42.5°C while maintaining the same heating time, TC pretreatment greatly increased the cell viability to 83% of the control value under H_2O_2 stress, while the HT group only exhibited a slight increase (Fig 2C). When we further increased the heating time to 3 h, the treatment of HT alone was cytotoxic to the cells, reducing the cell viability to 75.4%, and the viability was even lower after the H_2O_2 treatment (Fig 2C). Interestingly, the TC treatment with the same total thermal dose (12 cycles) had only a slight influence on the cell viability, and it still conferred significant neuroprotective effect to the SH-SY5Y cells under H_2O_2 stress.

In particular, the study examined the influence of the cooling process on the neuroprotective effect. As shown in Fig 2D, for low temperature period longer than 1 min, the TC pretreatment did not produce protective effect to the cells, indicating that the low temperature period is a critical parameter to be determined for effective neuroprotection. From molecular point of view, the neuroprotective effect would be discontinued as long as there were at least one or few critical signalling pathways being blocked as heating was halted, so we found that the low temperature period used for effective protection was shorter than the heating time in TC-HT treatment. On the other hand, the LDH release rate was measured and found to decrease significantly in the TC pretreatment group compared to the H_2O_2-treated group (Fig 2E), further confirming its protective role in maintaining the cell membrane integrity when cell was under oxidative stress. For AD disease model, Aβ treatment was used to reduce the viability of SH-SY5Y cells due to the cytotoxicity of the aggregated Aβ (Fig 3A). Our results showed that the TC treatment after Aβ administration greatly improved the viability of SH-SY5Y cells (Fig 3B) for nearly 25%, indicating the curative effect of TC in AD disease model in vitro. The most effective high temperature setting was 42.3°C for 8 cycles in the Aβ-treated cells. The actual high temperature sensed by the cells was about 41.7°C. Interestingly, the curative effect of TC pretreatment was less pronounced than that of TC post-treatment (treated after Aβ

administration), indicating the time point of TC application has great impact on the curative effect. Moreover, there were no curative effects by both HT pretreatment and post-treatment on SH-SY5Y cells, whose viability levels were of no difference with that in the Aβ only group (Fig 3B), implying the toxicity of Aβ was not attenuated by heat treatment. Thus, the results confirmed the therapeutic effect of TC-HT in AD disease model in vitro. Furthermore, the light microscopy images showed that the integrity of the cells was destructed by Aβ, and the TC treatment caused the protective effect to retain the cell morphology, as shown in Fig 3C.

To conclude the result of the H_2O_2-induced oxidative stress on SH-SY5Y cells, the protective effect of TC pretreatment was more pronounced than the HT preconditioning. And the TC pretreatment at 42.5°C produced much superior protection effect than at 41.5°C. Noteworthily, the HT pretreatment at 42.5°C for 3 h decreased the cell viability which indicates that the continuous heating may induce cell damage. The protective effect of TC was most remarkable at ~42.5°C for 8 cycles. Therefore, we chose this parameter to evaluate the possible protective mechanism of TC-HT in the following experiments.

Fig 2. Effect of TC-HT on H_2O_2-induced cytotoxicity in SH-SY5Y cells. (A) Dose-response curve of SH-SY5Y cells treated with different concentrations of H_2O_2

for 24 h. (B) SH-SY5Y cells were pretreated at 41.5°C temperature setting and challenged with or without 450 μM H_2O_2. The cell viability was measured by MTT assay at 24 h after the H_2O_2 treatment. (C) SH-SY5Y cells were pretreated at 42.5°C temperature setting with different thermal dosages and challenged with or without 450 μM H_2O_2. The cell viability was measured by MTT assay at 24h after the H_2O_2 treatment. (D) Comparison of the neuroprotective effect under different low temperature period settings. (E) The LDH release was measured to confirm the neuroprotective effect of TC treatment. SH-SY5Y cells were pretreated at 42.5°C temperature setting and challenged with or without 450 μM H_2O_2. The LDH release was measured 24h after the H_2O_2 treatment. Data represent the mean ± standard deviation (n=3). $^{***}P < 0.001$ and $^{**}P < 0.01$.

Fig 3. Effect of TC-HT on Aβ-induced cytotoxicity in SH-SY5Y cells. (A) The cell viability of SH-SY5Y cells treated with 25 or 50 μM Aβ for 4 days. (B) The TC or HT pretreatment and post-treatment at 42.5°C temperature setting were applied to the cells before or after 50 μM Aβ administration, and the cell viability was measured by MTT assay 4 days after treatment. The TC or HT treatment was applied 4 h before the Aβ administration for the pretreatment group and 1 h after Aβ administration for the post-treatment group. (C) Representative light microscopy images of SH-SY5Y cells

after treatment. The integrity of the cells was destructed by Aβ, and the TC post-treatment caused the protective effect and retained the cell morphology. Scale bar = 100 μm. Data represent the mean ± standard deviation (n=3). $^{***}P < 0.001$.

TC-HT attenuates H_2O_2-induced ROS generation

The onset and progression of AD has been reported to be associated with ROS. We further studied whether the H_2O_2-induced intracellular ROS production could be attenuated by the TC pretreatment. The intracellular ROS levels were detected using the fluorescent dye DHE (Fig 4A). Results showed that after exposure to 450 μM H_2O_2 for 24 h, ROS level was increased to 160% of the control value. When the SH-SY5Y cells were pretreated with TC-HT, the intracellular ROS level was significantly ameliorated (Fig 4B). Compared to the TC group, the ROS level was not changed in the HT group.

Fig 4. Effect of TC-HT on H_2O_2-induced ROS generation in SH-SY5Y cells. (A) ROS level was measured 24 h after the H_2O_2 treatment by flow cytometry with DHE fluorescent dye. (B) Quantification of the ROS levels after H_2O_2, TC+H_2O_2, or HT+H_2O_2 treatment. Data represent the mean ± standard deviation (n=3). $^{**}P < 0.01$.

TC-HT attenuates MMP loss in H_2O_2-treated cells

Many lines of evidence have suggested that mitochondria contribute to ageing-related neurodegenerative diseases through the accumulation of net cytosolic ROS production [21]. The levels of MMP are kept relatively stable in healthy cells. Apoptotic signals are usually initiated by the disruption of normal mitochondrial function, especially the collapse of MMP. To study the mechanism why H_2O_2-induced apoptosis is alleviated by TC-HT pretreatment, the MMP is further analyzed by the flow cytometry with $DiOC_6(3)$ fluorescent dye in the study. As shown in Fig 5A, the oxidative stress induced by H_2O_2 caused mitochondrial dysfunction, decreasing the MMP and therefore decreased the intensity of the $DiOC_6(3)$ fluorescent signal. From the quantification results (Fig 5B), it was found that the percentage of cells with decreased MMP drastically increased after the H_2O_2 treatment. In contrast to the group of H_2O_2 alone, the TC-HT pretreatment noticeably suppressed the H_2O_2-induced dissipation of MMP, so the cells with decreased MMP reduced significantly, which was attributed to the preservation of the mitochondrial function and thus caused the blockage of the apoptotic signaling transduction.

Fig 5. Effect of TC-HT on H_2O_2-induced MMP reduction in SH-SY5Y cells. (A) MMP was analyzed 24 h after the H_2O_2 treatment by flow cytometry with $DiOC_6(3)$

346 fluorescent dye. (B) Quantification of the cells with decreased MMP after H_2O_2,
347 TC+H_2O_2, or HT+H_2O_2 treatment. Data represent the mean ± standard deviation
348 (n=3). $^{***}P < 0.001$ and $^{**}P < 0.01$.
349

350 Effect of heat treatment on heat shock protein (HSP) 351 expressions in SH-SY5Y cells

352 It has been well known that HT triggers expression of HSPs so that cells are able
353 to protect themselves from stress [22, 23]. To investigate whether the protective effect
354 of TC-HT was related to the HSPs, we examined the protein expressions of HSP70
355 and HSP105, both of which were reported to have protective effects. As shown in Fig
356 6, both HSP expressions were enhanced significantly after HT and TC treatments. The
357 activation levels of TC, however, was only slightly higher than HT without significant
358 difference. This phenomenon points out that although TC treatment indeed protects
359 SH-SY5Y cells more from the oxidative stress of H_2O_2, the main mechanism could be
360 apart from the HSP70 or HSP105. Therefore, other heat-activated stress response
361 proteins should be considered in the experiments.
362

363 **Fig 6. Effect of TC-HT on expressions of HSPs in SH-SY5Y cells.** (A) Cells were
364 lysed 16 h after H_2O_2 treatment and western blot analyses of HSP70 and HSP105

365 expressions were performed. (B) Quantification of HSP70 and HSP105 expressions
366 after H_2O_2, TC+H_2O_2, or HT+H_2O_2 treatment. The expression levels were normalized
367 to GAPDH. Data represent the mean ± standard deviation (n=3). $^{***}P < 0.001$.
368

369 Effect of heat treatment on insulin-degrading enzyme and 370 proteasome expressions in SH-SY5Y cells

371 Insulin-degrading enzyme (IDE) is a highly conserved zinc metallopeptidase
372 which was originally identified as the key enzyme for the degradation of insulin.
373 Further studies unraveled its ability to degrade several other polypeptides, including
374 Aβ [24]. Recent studies demonstrated that IDE was up-regulated in a HSP-like
375 fashion [25]. In this study, we also examine the expression levels of IDE under the TC
376 or HT treatment. The results showed that H_2O_2 significantly decreased the expression
377 level of IDE and the heat treatment by TC remarkably recovered its expression level
378 while HT had notably weaker ability to regain the normal condition. Another
379 important protein quality control system which could degrade the Aβ peptide is the
380 ubiquitin-proteasome system (UPS). Regulation of Aβ production by the UPS may
381 have a role in AD pathogenesis and therefore the UPS is regarded as potential
382 therapeutic target for AD [26]. The proteasome comprises a proteolytic 20S core
383 particle capped by either one or two 19S regulatory particles. In this study, the protein

expression levels of 20S (PSMA3) and 19S (PSMC3) subunits were examined to verify the effect of thermal treatment on proteasome expression. The results showed that both expressions of PSMC3 and PSMA3 were weakened by H_2O_2 significantly. For the thermal treatment by TC, the levels of PSMC3 and PSMA3 expressions were greatly recovered especially in the PSMA3 level (return to 80% of the control value). For the HT treatment group, the degree of recovery was much lower than TC treatment group in both PSMC3 and PSMA3 expressions, while it had no significant difference compared to the H_2O_2-treated group in PSMA3 protein expressions.

Fig 7. Effect of TC-HT on expressions of IDE and proteasome in SH-SY5Y cells. (A) Cells were lysed 15 h after H_2O_2 treatment and western blot analyses of IDE and proteasome subunits (PSMC3 and PSMA3) expressions were performed. (B) Quantification of IDE, PSMC3, and PSMA3 expressions after H_2O_2, TC+H_2O_2, or HT+H_2O_2 treatment. The expression levels were normalized to GAPDH. Data represent the mean ± standard deviation (n=3). $^{***}P < 0.001$ and $^{**}P < 0.01$.

Effect of heat treatment on Akt-Nrf2/CREB signalling pathways in H_2O_2-treated SH-SY5Y cells

We then examined the signalling pathways that could participate in the

neuroprotective mechanism of TC-HT. The Akt pathway is highly conserved in all cells of higher eukaryotes and plays pivotal roles in cell survival and growth. Once Akt is activated by phosphorylation, it positively regulates some transcription factors to allow expression of prosurvival proteins. Therefore, in our study, we examined the phosphorylation of Akt and the downstream transcription factors including cAMP response element binding protein (CREB) and nuclear factor erythroid 2-related factor 2 (Nrf2) by western blot analysis. As shown in Fig 8, the expression of phosphorylated Akt (p-Akt) was increased in H_2O_2-treated SH-SY5Y cells compared to the untreated cells. The increased p-Akt level could be due to the stress response induced by the oxidative stress of H_2O_2. Heat pretreatment further increased the p-Akt levels in H_2O_2-treated SH-SY5Y cells, and the TC group had significantly higher level of p-Akt than the HT group. We also examined the expression levels of p-CREB and Nrf2. CREB is an important transcription factor that also triggers expression of many prosurvival proteins, including Bcl-2 and brain derived neurotrophic factor (BDNF) [27]. When CREB is phosphorylated, it starts to regulate downstream gene expression. Besides, Nrf2 is also a key transcription factor that regulates expression of antioxidant proteins, such as heme oxygenase-1 (HO-1) [28]. As shown in Fig 8, H_2O_2 treatment slightly influenced Nrf2 and p-CREB protein expression levels. In the heat-treated groups, the TC treatment significantly increased the expressions of Nrf2

and p-CREB, while the HT treatment increased Nrf2 expression with less significant level than TC treatment but in turn reduced the expression level of p-CREB. The HO-1 protein is a heme-containing HSP which is crucial for neuroprotection against oxidative stress. The result showed that the heat treatment significantly enhanced the expression levels of HO-1 in TC and HT groups. Particularly, it is worth noting that the TC treatment had a significant higher level of HO-1 than HT, which could account for the antioxidant ability of the TC treatment in the ROS experiment.

Fig 8. Effect of TC-HT on Akt/Nrf2 and Akt/CREB signalling pathways and related protein expressions. Cells were lysed 15 h after H_2O_2 treatment for p-Akt, Akt, Nrf2, p-CREB proteins, and lysed 18 h after H_2O_2 treatment for HO-1 protein, and western blot analyses of p-Akt, Akt, Nrf2, p-CREB, and HO-1 proteins were performed. Quantification of p-Akt, Nrf2, p-CREB, HO-1 expressions after H_2O_2, TC+H_2O_2, or HT+H_2O_2 treatment. The expression level of p-Akt was normalized to total Akt while other proteins were normalized to GAPDH. Data represent the mean ± standard deviation (n=3). $^{***}P < 0.001$, $^{**}P < 0.01$ and $^{*}P < 0.05$.

Effect of LY294002 on the TC-HT activated Akt pathway and protective effect

441 In order to examine if the activation of the Akt pathway was involved in the
442 neuroprotective effect of TC treatment, we inhibited the phosphoinositide-3-kinase
443 (PI3K), the upstream kinase of Akt, by the inhibitor LY294002 [29] in the study. In
444 Fig 9A, we found that H_2O_2 treatment reduced the viability of SH-SY5Y cells to 58%
445 of the control value, and TC treatment could greatly increase the cell viability to
446 ~86% of the control value under H_2O_2 stress. In the presence of PI3K inhibitor, the
447 p-Akt level was indeed reversed and the neuroprotective effect of TC treatment
448 against H_2O_2-induced cell apoptosis was abrogated (Fig 9A and 9B), representing that
449 the Akt pathway was involved to mediate the neuroprotective effect of TC treatment
450 against H_2O_2 toxicity. For the downstream proteins of Akt, inhibition of the PI3K/Akt
451 pathway was found to significantly reduce the induction of Nrf2 by TC treatment,
452 indicating that the transcription factor Nrf2 was indeed activated by the Akt pathway.
453 Collectively, these data point out that TC treatment may exhibit neuroprotective effect
454 via activation of the Akt-Nrf2/CREB signalling pathways in the H_2O_2-treated
455 SH-SY5Y neuron cells.
456
457 **Fig 9. Effect of LY294002 on the neuroprotective effect of TC-HT and related**
458 **protein expressions.** (A) TC treatment conferred neuroprotective effect and
459 significantly increased the cell viability of SH-SY5Y neuron cells under the H_2O_2

stress. The neuroprotective effect of TC treatment was abrogated by addition of the PI3K inhibitor LY294002 in a dose-dependent manner. (B) Cells were lysed 15 h after H_2O_2 or 25 μM LY294002 treatment, and western blot analyses of p-Akt and Nrf2 proteins were performed. The inhibitor LY294002 reversed the activated levels of p-Akt and Nrf2 induced by TC treatment. The expression level of p-Akt and Nrf2 was normalized to total Akt and GAPDH, respectively. We used the abbreviation "LY" to represent the PI3K inhibitor LY294002 in the figure. Data represent the mean ± standard deviation (n=3). $^{***}P < 0.001$, $^{**}P < 0.01$ and $^{*}P < 0.05$.

Discussion

The study focused on investigating the neuroprotective effect of TC-HT on SH-SY5Y cells. It showed that subjection of the cells to heat at high and low temperatures alternately could produce significant protective effect against H_2O_2 and Aβ-induced apoptosis in SH-SY5Y human neural cells. The western blot results showed that TC-HT activated the PI3K/Akt signalling pathway and mediated the activation of Nrf2 and CREB proteins.

A human derived cell line SH-SY5Y has been extensively employed as general in vitro model in evaluating neuronal damage or neurodegenerative diseases, such as

AD and PD [30, 31]. Therefore, the study used SH-SY5Y cells in the experiments to determine the protective effect of TC-HT against H_2O_2 and Aβ-induced cytotoxicity. Although the exact molecular mechanism of neurodegeneration pathogenesis is still not clear, a common feature of these diseases is oxidative stress [32]. Many researchers believe that oxidative stress may play a critical role in the etiology and cause the exacerbation of disease progression. Cellular ROS are generated by both extrinsic and intrinsic sources, with the former including ultraviolet, drugs, and environmental toxins. Under normal physiological conditions, ROS generated intrinsically from mitochondria and other enzymes are maintained at appropriate levels by endogenous antioxidants. However, when mitochondria suffers from decreased antioxidant defense or cell inflammation due to damage, excess ROS production may occur. Since neuron cells are especially vulnerable to oxidative damage due to their high oxygen demand and high polyunsaturated fatty acid contents in membranes [33], the imbalance between ROS production and removal may cause neuron damage or degeneration. A key cellular and molecular mechanism of several neurodegenerative diseases, such as AD, PD, Huntington's disease (HD), amyotrophic lateral sclerosis (ALS), is the accumulation of misfolded aggregation proteins in brain [34]. The deposition of these misfolded protein aggregates can cause inflammation in brain, inducing significant ROS production and leading to synaptic dysfunction,

498 neuronal apoptosis, and brain degeneration [35]. The composition of protein
499 aggregates is different among various neurodegenerative diseases. For AD, there are
500 two main kinds of protein aggregates, namely extracellular amyloid plaques deriving
501 from amyloid precursor protein and intracellular microtubule-associated protein tau,
502 known as neurofibrillary tangles [36]. With the complex pathogeneses of Aβ or tau
503 proteins still remaining largely unknown, several studies have proven that the
504 accumulation of Aβ increased oxidative stress and led to mitochondrial dysfunction
505 and DNA/RNA oxidation [37]. Matsuoka et al. showed that AD transgenic mouse
506 with Aβ accumulation can cause an increase in H_2O_2 level, suggesting that Aβ may
507 enhance oxidative stress in AD [38]. The oxidative stress can boost the
508 hyper-phosphorylation of tau protein and in turn facilitate the aggregation of Aβ [39].
509 Studies have also pointed out that overexpressed tau proteins make the cells more
510 vulnerable to oxidative stress [40]. Therefore, efforts have been underway to find
511 therapeutic strategies that can protect against oxidative stress and alleviate the
512 symptoms of neurodegenerative diseases. Among numerous ROS species, H_2O_2 can
513 be considered to be one of the most important ROS molecules involved in the
514 progression of AD. Many studies, therefore, used H_2O_2 to induce oxidative stress in
515 vitro, as a model in the investigation of the neuroprotective or neurodamage
516 mechanisms [41-43]. The study also found that H_2O_2 increased the ROS level in

517 SY-SY5Y cells and caused the cell death in a dose-dependent manner. Additionally,
518 Aβ was used to further investigate the neuroprotective effect of TC-HT in the AD
519 disease model. Both MTT and LDH release assays were employed in assessing the
520 neuroprotective effect of TC-HT. The results showed that TC-HT increased the cell
521 viability in the H_2O_2 and Aβ-treated neural cells. The detection of ROS level showed
522 that one possible mechanism of neuroprotective action of TC-HT exhibited the
523 antioxidant property, reducing the intracellular ROS level, perhaps due to the increase
524 of antioxidant enzymes in SH-SY5Y cells, induced by TC-HT. In the western blot
525 results, the study proved that such effect was through activation of Akt/Nrf2 pathway.
526 The Akt signaling pathway is a key regulator in the survival, proliferation, and
527 migration of cells, in response to extracellular signals [44]. Phosphorylation of Akt
528 further activates a set of downstream transcription factors, including Nrf2 and CREB,
529 which are considered to be mediators of neuroprotection by increasing the expression
530 of many antioxidant and prosurvival enzymes under oxidative stress. Nrf2 is one of
531 the most important transcription factors that regulate the expression of various
532 antioxidant proteins and maintain the redox state in mammalian cells [45, 46]. Among
533 various antioxidant proteins, HO-1 has been proven to be effective in promoting
534 antioxidant production and protection against neuronal injury [28]. The study found
535 that the physical stimulation, TC-HT, could activate the Akt/Nrf2 pathway and

upregulate the expression of the antioxidant protein HO-1, thereby reducing the ROS generation by H_2O_2. Compared with the continuous heating of HT group, TC-HT performed significantly better in activating Akt/Nrf2, HO-1 expression, and ROS reduction, in agreement with the cell viability assay.

Another possible mechanism for neuroprotection of TC-HT may be related to the activation of Akt/CREB pathway. CREB is the cellular transcription factor activated by phosphorylation from Akt or other kinases, which triggers expression of neurotrophins and antiapoptotic proteins. The critical role of CREB in neuronal plasticity and long-term memory has also been well-documented [47]. In addition to the neuroprotective effect of CREB by upregulating neurotrophins and antiapoptotic proteins, recent studies have discovered that CREB also protects neurons via the antioxidant pathways [27]. The downstream antioxidant genes include HO-1 and manganese superoxide dismutase (MnSOD). Besides, CREB downregulation is involved in the pathology of AD [48], and thus increasing the expression of CREB has been considered a potential therapeutic strategy for AD [49]. In some preconditioning experiments, CREB seemed to play a key role in the preconditioning response which protected the cells from the subsequent stress [50]. In the study, it was observed that TC-HT pretreatment significantly upregulated the activation of CREB protein, compared with the control group in SH-SY5Y cells. The result further found

555 that HT significantly decreased the expression level of p-CREB compared with the
556 control cells. The decreased level of p-CREB in HT group indicates that HT may
557 exert too much heat stress and thus hinder the neuroprotective effect or even cause
558 damage to the cells. Taken together, the result points out that the neuroprotective
559 effect of TC-HT could be attributed to the function of antioxidant protein HO-1 or
560 other prosurvival proteins via activation of Nrf2 and CREB through PI3K/Akt
561 pathway (Fig 10). Further studies are necessary to identify the specific role of other
562 downstream neurotrophins and antiapoptotic or antioxidant proteins in the
563 neuroprotection effect.
564
565 **Fig 10. The proposed mechanisms for the protective effect of TC-HT against**
566 **H_2O_2 or Aβ-induced neural injury.** The epidermal growth factor receptor (EGFR) in
567 the cell membrane could be the upstream receptor sensing extracellular TC-HT
568 stimulation and transmit the signal to activate the PI3K/Akt pathway, which induces
569 Nrf2 and CREB activations. The transcription factors entering the nucleus further
570 enhance the expressions of HO-1 and other prosurvival proteins which decrease the
571 ROS level and inhibit the apoptosis signal.
572
573 Under stress amid a harsh environment or caused by external stimuli, cells or

574 whole organisms would trigger self-defense systems in response [51]. For example,
575 fever induced by viral or bacterial infections is a useful defense mechanism capable of
576 regulating the body temperature, as higher body temperature strengthens immune
577 cells and increases their ability to kill bacteria and viruses. It also inhibits the growth
578 of bacteria and viruses, thereby attaining anti-inflammatory effects. Depending on the
579 intensity and duration of stress, cells would activate cell repair or stress response to
580 adapt to the new environment or cause their death [52]. The stress response involves
581 the synthesis of some highly conserved proteins with protective function for cells [53].
582 For the thermal stress induced when cells or whole organisms are exposed to elevated
583 temperatures, they would respond by synthesizing an evolutionary highly conserved
584 family of proteins, known as HSPs [54]. The HS response is a universal phenomenon,
585 which appears in every tested organism. HSPs are named and classified, according to
586 their molecular weight. HSP70 (70 kilodaltons in size) is a typical group of HSPs,
587 which functions a molecular chaperone, to prevent the misfolding of nascent
588 polypeptide chains and facilitate refolding of misfolded proteins [22]. Many studies
589 have indicated that HSP70 sub-family is essential in protecting organisms from
590 various stresses [55]. The study also examined the effect of TC-HT and HT on the
591 expression of HSP70 and HSP105 [23], both of which have been reported to have
592 protective effects. The results showed that HT and TC-HT treatments enhanced the

593 expression of both HSPs significantly. However, the activation level of TC-HT was
594 only slightly higher than HT group, which could not explain the superior protective
595 effect of TC-HT compared to HT. Another novel HS-like protein, IDE, was identified
596 as the major Aβ degrading enzyme, and its protein expression level was found to
597 correlate negatively with the AD pathology [24]. Previous study had shown that IDE
598 expression was stress-inducible [25]. In the study, it was found that the TC treatment
599 greatly recovered the H_2O_2-induced IDE reduction, and the enhanced level was much
600 higher than HT treatment. Therefore, IDE could be one of the proteins participating in
601 the neuroprotective effect under Aβ administration.

602 The stress response enables cells to survive the stress-induced damage. Use of
603 cells' self-defense ability to adapt the stress environment or manipulation of the stress
604 response to increase the survival rate may be valuable in regenerative medicine or
605 disease curing. In fact, there have been examples involving preconditioning of cells
606 with non-lethal stress to minimize cell damage and improve the transplantation
607 outcome [56]. While there have been many experiments on thermotolerance and cell
608 survival [57], none have demonstrated the stress response in neuroprotection and
609 curation to the best of our knowledge. Besides, the challenge for the manipulation of
610 cellular stress response is how to fine-tune stress intensity and duration to suit specific
611 needs and prevent the stress-induced cell damage. The present study demonstrated a

612 delicate and efficient way to activate the stress response, leading to protection and
613 curation against H_2O_2 and Aβ-induced cytotoxicity on SH-SY5Y cells. The thermal
614 dosage was fine-tuned in a heat-and-cold cycling process, to maximize the protective
615 effect and minimize the heat stress-induced cell damage. Although traditional HS can
616 activate HSPs which may provide resistance to insults, such as hyperthermia, the
617 continuous exposure may cause cell damage or even death. Previous studies have
618 shown that the threshold for thermal damage is different among various tissue cells,
619 which have different levels of thermal sensibility [58]. For example, the skin cells can
620 withstand much higher thermal dosage (47°C for 20 min) than neural cells, because
621 the neural cells are more vulnerable. As the most thermally sensitive tissue, brain can
622 be damaged by low thermal dosage [58]. To attain optimal thermal dosage for various
623 tissues, the heating process should be divided into several parts, which is the basic
624 architecture of TC-HT.

625 In this study, the work presented an efficient and guaranteed way of controlling
626 the thermal dosage applied to cells. The novelty of the TC-HT strategy is periodically
627 interspersing the short period of cooling process in the continuous heating HT
628 treatment. The body temperature (37°C) was selected as the low temperature setting
629 which mimics the passive cooling process in the human body. Interestingly, our data
630 demonstrated that the application time of the low temperature period is a critical

parameter to determine the efficacy of neuroprotection for TC-HT. For too short cooling period, the accumulation of the thermal dosage will cause damage to neural cells like HT. On the other side, it was found that the TC-HT did not produce protective effect to the cells when low temperature period was longer than 1 min (Fig 2D). It may be due to the reason that the application of too long cooling period (> 1 min) could interrupt the transmission of biochemical signals and protein expressions stimulated by thermal stress, thus failing to achieve the neuroprotective effect. The results revealed that 35 sec cooling process at 37°C after 15 min heating at 42.5°C for 8 cycles produces the optimum protective effect to SH-SY5Y cells. This protective effect employing TC-HT was significantly much better than the continuous HT, which was due to the activation of other thermal stress-associated proteins apart from HSPs and the prevention of heat damage. From the LY294002 experiment, it was confirmed that the superior protective effect resulted partially from the activation of Akt pathway. One fascinating phenomenon is the antioxidant effect induced by TC-HT, which could be attributed to the increased antioxidant protein HO-1. Besides, the Aβ-induced cytotoxicity was also rescued in TC-HT treated cells, which points out the possibility that some stress-induced proteins might have the ability to eliminate or refold the aggregated protein or ease the symptom at least. The chaperone or proteasome systems are possible candidates to be involved in this phenomenon [59]. Actually,

previous studies had shown that IDE will interact with 20S proteasome and modulate its proteolytic activity [60]. Our results showed that TC treatment could not only enhance the expression of IDE but also increase the proteasome expressions of 20S (PSMA3) and 19S (PSMC3) subunits. Although the examination was performed for only one subunit of the 20S and 19S particles, respectively, one could not rule out the possibility that TC treatment increased the abundance of proteasome complexes. Further studies are needed to confirm if the proteolytic activity of 20S proteasome is increased by the TC treatment and thus facilitates the degradation of Aβ polypeptides.

It is noteworthy that TC-HT applied after the Aβ administration gives better curative effect than the pretreatment paradigm, which indicates that TC-HT not only has the ability to prevent or protect the neurons against the Aβ-induced cytotoxicity but also could have the potential to cure the disease. The possible explanation for the superior effect of post-treatment could be that some biochemical signals and elevated proteins could interact with the Aβ aggregation simultaneously, and these effects could not maintain until the insult for the pretreated cells. Another advantage is that the post-treatment paradigms for neuronal injury are also more typical in the clinical condition. The present study employed PCR equipment to demonstrate the protective effect of TC-HT in vitro. For in vivo or clinical applications, there are options of other heating devices, such as high-intensity focused ultrasound (HIFU), which has been

669 widely used as a hyperthermal apparatus [61]. The thermal parameters can also be
670 fine-tuned by controlling the heating power and the size of heated volume to meet the
671 specific needs [62].

672 In summary, this is the first study on the manipulation of stress response by
673 TC-HT, which protects SH-SY5Y human neural cells from H_2O_2 and Aβ-induced
674 cytotoxicity. The results confirm that the physical stimulation by TC-HT provides
675 safer and much superior protective effect than continuous HS. The underlying
676 molecular mechanism for the protective effect is partially due to the activation of Akt
677 pathway and the function of some downstream proteins, such as Nrf2, CREB, and
678 HO-1. Further studies are necessary to confirm the involvement of other
679 stress-induced proteins activated by TC-HT in the neuroprotective effect or their
680 ability in degrading or disaggregating the aggregated proteins. It is also advisable for
681 coupling TC-HT with NDD drugs or natural compounds, in order to attain better
682 curative effect for NDD patients.

683

684 # Funding

685 This work was supported by grants from Ministry of Science and Technology
686 (MOST 108-2112-M-002-016 and 105-2112-M-002-006-MY3 to CYC) and Ministry
687 of Education (MOE 106R880708 to CYC) of the Republic of China. The funders had

688 no role in study design, data collection and analysis, decision to publish, or
689 preparation of the manuscript.

690

691 Competing Interests

692 The authors have declared that no competing interests exist.

693

694 Acknowledgments

695 The authors would like to acknowledge the service provided by the Research
696 Core Facilities 3 Laboratory of the Department of Medical Research at National
697 Taiwan University hospital for use of flow cytometry system.

698

699 Author Contributions

700 **Conceptualization:** Chih-Yu Chao.

701 **Data Curation:** Wei-Ting Chen, Yu-Yi Kuo, Guan-Bo Lin, Chih-Yu Chao.

702 **Formal analysis:** Wei-Ting Chen, Yu-Yi Kuo, Guan-Bo-Lin, Chueh-Hsuan Lu,
703 Hao-Ping Hsu, Yi-Kun Sun, Chih-Yu Chao.

704 **Funding acquisition:** Chih-Yu Chao.

705 **Investigation:** Wei-Ting Chen, Yu-Yi Kuo, Guan-Bo Lin, Chih-Yu Chao.

706 **Project Administration:** Chih-Yu Chao.

Supervision: Chih-Yu Chao.

Validation: Wei-Ting Chen, Yu-Yi Kuo, Guan-Bo Lin.

Writing – original draft: Wei-Ting Chen, Yu-Yi Kuo, Chih-Yu Chao.

Writing – review & editing: Chih-Yu Chao.

References:

1. Kim GH, Kim JE, Rhie SJ, Yoon S. The role of oxidative stress in neurodegenerative diseases. Exp Neurobiol. 2015; 24:325-340.
2. Finkel T, Holbrook NJ. Oxidants, oxidative stress and the biology of ageing. Nature. 2000; 408:239-247.
3. Liu Z, Zhou T, Ziegler AC, Dimitrion P, Zuo L. Oxidative stress in neurodegenerative diseases: from molecular mechanisms to clinical applications. Oxidative Med Cell Longev. 2017; 2017:2525967.
4. Bachurin SO, Bovina EV, Ustyugov AA. Drugs in clinical trials for Alzheimer's disease: the major trends. Med Res Rev. 2017; 37:1186-1225.
5. Alghazwi M, Smid S, Musgrave I, Zhang W. In vitro studies of the neuroprotective activities of astaxanthin and fucoxanthin against amyloid beta (Aβ1-42) toxicity and aggregation. Neurochem Int. 2019; 124:215-224.
6. Hemming ML, Selkoe DJ. Amyloid beta-protein is degraded by cellular angiotensin-converting enzyme (ACE) and elevated by an ACE inhibitor. J Biol Chem. 2005; 280:37644-37650.
7. Yang Y, Zhang X, Ye D, Laforest R, Williamson J, Liu Y, et al. Cavitation dose painting for focused ultrasound-induced blood-brain barrier disruption. Sci Rep. 2019; 9:2840.
8. Habash RW, Bansal R, Krewski D, Alhafid HT. Thermal therapy, part 1: an introduction to thermal therapy. Crit Rev Biomed Eng. 2006; 34:459-489.
9. Christophi C, Winkworth A, Muralihdaran V, Evans P. The treatment of malignancy by hyperthermia. Surg Oncol. 1998; 7:83-90.
10. Schaaf L, Schwab M, Ulmer C, Heine S, Mürdter TE, Schmid JO, et al. Hyperthermia synergizes with chemotherapy by inhibiting PARP1-dependent DNA replication arrest. Cancer Res. 2016; 76:2868-2875.
11. Lord-Fontaine S, Averill-Bates DA. Heat shock inactivates cellular antioxidant

739 defenses against hydrogen peroxide: protection by glucose. Free Radic Biol Med.
740 2002; 32:752-765.
741 12. Tchouagué M, Grondin M, Glory A, Averill-Bates D. Heat shock induces the
742 cellular antioxidant defenses peroxiredoxin, glutathione and glucose 6-phosphate
743 dehydrogenase through Nrf2. Chem-Biol Interact. 2019; 310:108717.
744 13. Mustafi SB, Chakraborty PK, Dey RS, Raha S. Heat stress upregulates
745 chaperone heat shock protein 70 and antioxidant manganese superoxide dismutase
746 through reactive oxygen species (ROS), p38MAPK, and Akt. Cell Stress Chaperones.
747 2009; 14:579-589.
748 14. Hamblin MR. Shining light on the head: photobiomodulation for brain disorders.
749 BBA clinical. 2016; 6:113-124.
750 15. Chen WT, Sun YK, Lu CH, Chao CY. Thermal cycling as a novel thermal
751 therapy to synergistically enhance the anticancer effect of propolis on PANC-1 cells.
752 Int J Oncol. 2019; 55:617-628.
753 16. Lu CH, Chen WT, Hsieh CH, Kuo YY, Chao CY. Thermal cycling-hyperthermia
754 in combination with polyphenols, epigallocatechin gallate and chlorogenic acid,
755 exerts synergistic anticancer effect against human pancreatic cancer PANC-1 cells.
756 PLoS One. 2019; 14:e0217676.
757 17. Sminia P, Zee JVD, Wondergem J, Haveman J. Effect of hyperthermia on the
758 central nervous system: a review. Int J Hyperthermia. 1994; 10:1-30.
759 18. Son SM, Kang S, Choi H, Mook-Jung I. Statins induce insulin-degrading
760 enzyme secretion from astrocytes via an autophagy-based unconventional secretory
761 pathway. Mol Neurodegener. 2015; 10:56.
762 19. Deane CAS, Brown IR. Induction of heat shock proteins in differentiated human
763 neuronal cells following co-application of celastrol and arimoclomol. Cell Stress
764 Chaperones. 2016; 21:837-848.
765 20. Jin X, Xu Z, Cao J, Yan R, Xu R, Ran R, et al. HO-1/EBP interaction alleviates
766 cholesterol-induced hypoxia through the activation of the AKT and Nrf2/mTOR
767 pathways and inhibition of carbohydrate metabolism in cardiomyocytes. Int J Mol
768 Med. 2017; 39:1409-1420.
769 21. Lin MT, Beal MF. Mitochondrial dysfunction and oxidative stress in
770 neurodegenerative diseases. Nature. 2006; 443:787-795.
771 22. Mosser DD, Caron AW, Bourget L, Meriin AB, Sherman MY, Morimoto RI, et al.
772 The chaperone function of hsp70 is required for protection against stress-induced
773 apoptosis. Mol Cell Biol. 2000; 20:7146-7159.
774 23. Hatayama T, Yamagishi N, Minobe E, Sakai K. Role of hsp105 in protection
775 against stress-induced apoptosis in neuronal PC12 cells. Biochem Biophys Res
776 Commun. 2001; 288:528-534.

24. Tundo GR, Sbardella D, Ciaccio C, Grasso G, Gioia M, Coletta A, et al. Multiple functions of insulin-degrading enzyme: a metabolic crosslight? Crit Rev Biochem Mol Biol. 2017; 52:554-582.

25. Tundo GR, Sbardella D, Ciaccio C, Bianculli A, Orlandi A, Desimio MG, et al. Insulin-degrading enzyme (IDE): A novel heat shock-like protein. J Biol Chem. 2013; 288:2281-2289.

26. Gong B, Radulovic M, Figueiredo-Pereira ME, Cardozo C. The ubiquitin-proteasome system: potential therapeutic targets for Alzheimer's disease and spinal cord injury. Front Molec Neurosci. 2016; 9:4.

27. Sakamoto K, Karelina K, Obrietan K. CREB: a multifaceted regulator of neuronal plasticity and protection. J Neurochem. 2011; 116:1-9.

28. Wang Z, Guo S, Wang J, Shen Y, Zhang J, Wu Q. Nrf2/HO-1 mediates the neuroprotective effect of mangiferin on early brain injury after subarachnoid hemorrhage by attenuating mitochondria-related apoptosis and neuroinflammation. Sci Rep. 2017; 7:11883.

29. Sanchezmargalet V, Goldfine ID, Vlahos CJ, Sung CK. Role of phosphatidylinositol-3-kinase in insulin receptor signaling: studies with inhibitor, LY294002. Biochem Biophys Res Commun. 1994; 204:446-452.

30. Wu X, Kosaraju J, Zhou W, Tam KY. Neuroprotective effect of SLM, a novel carbazole-based fluorophore, on SH-SY5Y cell model and 3xTg-AD mouse model of Alzheimer's disease. ACS Chem Neurosci. 2017; 8:676-685.

31. Xicoy H, Wieringa B, Martens GJ. The SH-SY5Y cell line in Parkinson's disease research: a systematic review. Mol Neurodegener. 2017; 12:10.

32. Barnham KJ, Masters CL, Bush AI. Neurodegenerative diseases and oxidative stress. Nat Rev Drug Discov. 2004; 3:205-214.

33. Chen X, Guo C, Kong J. Oxidative stress in neurodegenerative diseases. Neural Regen Res. 2012; 7:376-385.

34. Ross CA, Poirier MA. Protein aggregation and neurodegenerative disease. Nat Med. 2004; 10:S10-S17.

35. Masters SL, O'Neill LAJ. Disease-associated amyloid and misfolded protein aggregates activate the inflammasome. Trends Mol Med. 2011; 17:276-282.

36. Choi ML, Gandhi S. Crucial role of protein oligomerization in the pathogenesis of Alzheimer's and Parkinson's diseases. FEBS J. 2018; 285:3631-3644.

37. Manczak M, Anekonda TS, Henson E, Park BS, Quinn J, Reddy PH. Mitochondria are a direct site of Aβ accumulation in Alzheimer's disease neurons: implications for free radical generation and oxidative damage in disease progression. Hum Mol Genet. 2006; 15:1437-1449.

38. Matsuoka Y, Picciano M, La Francois J, Duff K. Fibrillar β-amyloid evokes

oxidative damage in a transgenic mouse model of Alzheimer's disease. Neuroscience. 2001; 104:609-613.

39. Huang HC, Jiang ZF. Accumulated amyloid-β peptide and hyperphosphorylated tau protein: relationship and links in Alzheimer's disease. J Alzheimers Dis. 2009; 16:15-27.

40. Zhao Y, Zhao B. Oxidative stress and the pathogenesis of Alzheimer's disease. Oxidative Med Cell Longev. 2013; 2013:316523.

41. de Oliveira MR, de Bittencourt Brasil F, Fürstenau CR. Sulforaphane promotes mitochondrial protection in SH-SY5Y cells exposed to hydrogen peroxide by an Nrf2-dependent mechanism. Mol Neurobiol. 2017; 55:4777-4787.

42. Ismail N, Ismail M, Imam MU, Azmi NH, Fathy SF, Foo JB, et al. Mechanistic basis for protection of differentiated SH-SY5Y cells by oryzanol-rich fraction against hydrogen peroxide-induced neurotoxicity. BMC Complement Altern Med. 2014; 14:467.

43. Han SM, Kim JM, Park KK, Chang YC, Pak SC. Neuroprotective effects of melittin on hydrogen peroxide-induced apoptotic cell death in neuroblastoma SH-SY5Y cells. BMC Complement Altern Med. 2014; 14:286.

44. Jason S, Cui W. Proliferation, survival and metabolism: the role of PI3K/AKT/mTOR signalling in pluripotency and cell fate determination. Development. 2016; 143:3050-3060.

45. Huang Y, Li W, Su ZY, Kong ANT. The complexity of the Nrf2 pathway: beyond the antioxidant response. J Nutr Biochem. 2015; 26:1401-1413.

46. Kubben N, Zhang W, Wang L, Voss TC, Yang J, Qu J, et al. Repression of the antioxidant NRF2 pathway in premature aging. Cell. 2016; 165:1361-1374.

47. Caracciolo L, Marosi M, Mazzitelli J, Latifi S, Sano Y, Galvan L, et al. CREB controls cortical circuit plasticity and functional recovery after stroke. Nat Commun. 2018; 9:2250.

48. Rosa E, Fahnestock M. CREB expression mediates amyloid β-induced basal BDNF downregulation. Neurobiol Aging. 2015; 36:2406-2413.

49. Qin Z. Modulating nitric oxide signaling in the CNS for Alzheimer's disease therapy. Future Med Chem. 2013; 5:1451-1468.

50. Baranova KA, Rybnikova EA, Churilova AV, Vetrovoy OV, Samoilov MO. The adaptive role of the CREB and NF-κB neuronal transcription factors in post-stress psychopathology models in rats. Neurochem J. 2014; 8:17-23.

51. Chovatiya R, Medzhitov R. Stress, Inflammation, and defense of homeostasis. Mol Cell. 2014; 54:281-288.

52. Thomas MP, Lieberman J. Live or let die: posttranscriptional gene regulation in cell stress and cell death. Immunol Rev. 2013; 253:237-252.

53. Blanco S, Bandiera R, Popis M, Hussain S, Lombard P, Aleksic J, et al. Stem cell function and stress response are controlled by protein synthesis. Nature. 2016; 534:335-340.
54. Lindquist S. The heat-shock response. Annu Rev Biochem. 1986; 55:1151-1191.
55. Yenari MA, Liu J, Zheng Z, Vexler ZS, Lee JE, Giffard RG. Antiapoptotic and anti-inflammatory mechanisms of heat-shock protein protection. Ann NY Acad Sci. 2005; 1053:74-83.
56. Matsumoto K, Honda K, Kobayashi N. Protective effect of heat preconditioning of rat liver graft resulting in improved transplant survival. Transplantation. 2001; 71:862-868.
57. Mesihovic A, Iannacone R, Firon N, Fragkostefanakis S. Heat stress regimes for the investigation of pollen thermotolerance in crop plants. Plant Reprod. 2016; 29:93-105.
58. Dewhirst MW, Viglianti BL, Lora-Michiels M, Hanson M, Hoopes PJ. Basic principles of thermal dosimetry and thermal thresholds for tissue damage from hyperthermia. Int J Hyperthermia. 2003; 19:267-294.
59. Kampinga HH, Bergink S. Heat shock proteins as potential targets for protective strategies in neurodegeneration. Lancet Neurol. 2016; 15:748-759.
60. Sbardella D, Tundo GR, Coletta A, Marcoux J, Koufogeorgou EI, Ciaccio C, et al. The insulin-degrading enzyme is an allosteric modulator of the 20S proteasome and a potential competitor of the 19S. Cell Mol Life Sci. 2018; 75:3441-3456.
61. Frazier N, Payne A, de Bever J, Dillon C, Panda A, Subrahmanyam N, et al. High intensity focused ultrasound hyperthermia for enhanced macromolecular delivery. J Control Release. 2016; 241:186-193.
62. Partanen A, Tillander M, Yarmolenko PS, Wood BJ, Dreher MR, Kohler MO. Reduction of peak acoustic pressure and shaping of heated region by use of multifoci sonications in MR-guided high-intensity focused ultrasound mediated mild hyperthermia. Med Phys. 2013; 40:013301.

Figure 1

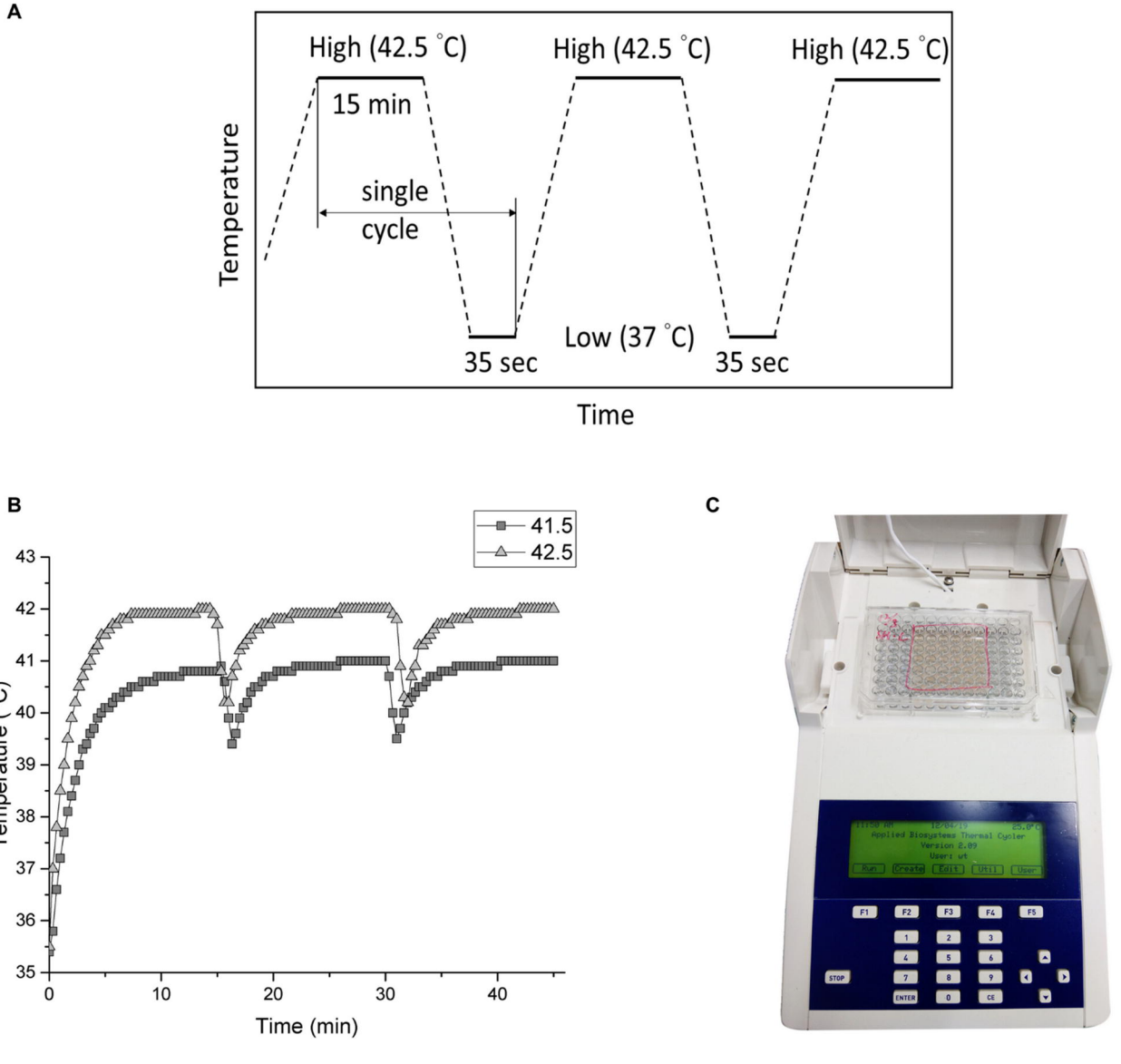
A
High (42.5 ˚C)
15 min
High (42.5 ˚C)
High (42.5 ˚C)
single
cycle
Temperature
35 sec
Low (37 ˚C)
35 sec
Time
B
41.5
42.5
Temperature (°C)
Time (min)
C
Applied Biosystems Thermal Cycler
Version 2.09
Run
Create
Edit
Util
User
F1
F2
F3
F4
F5
STOP
ENTER
CE

Figure 2

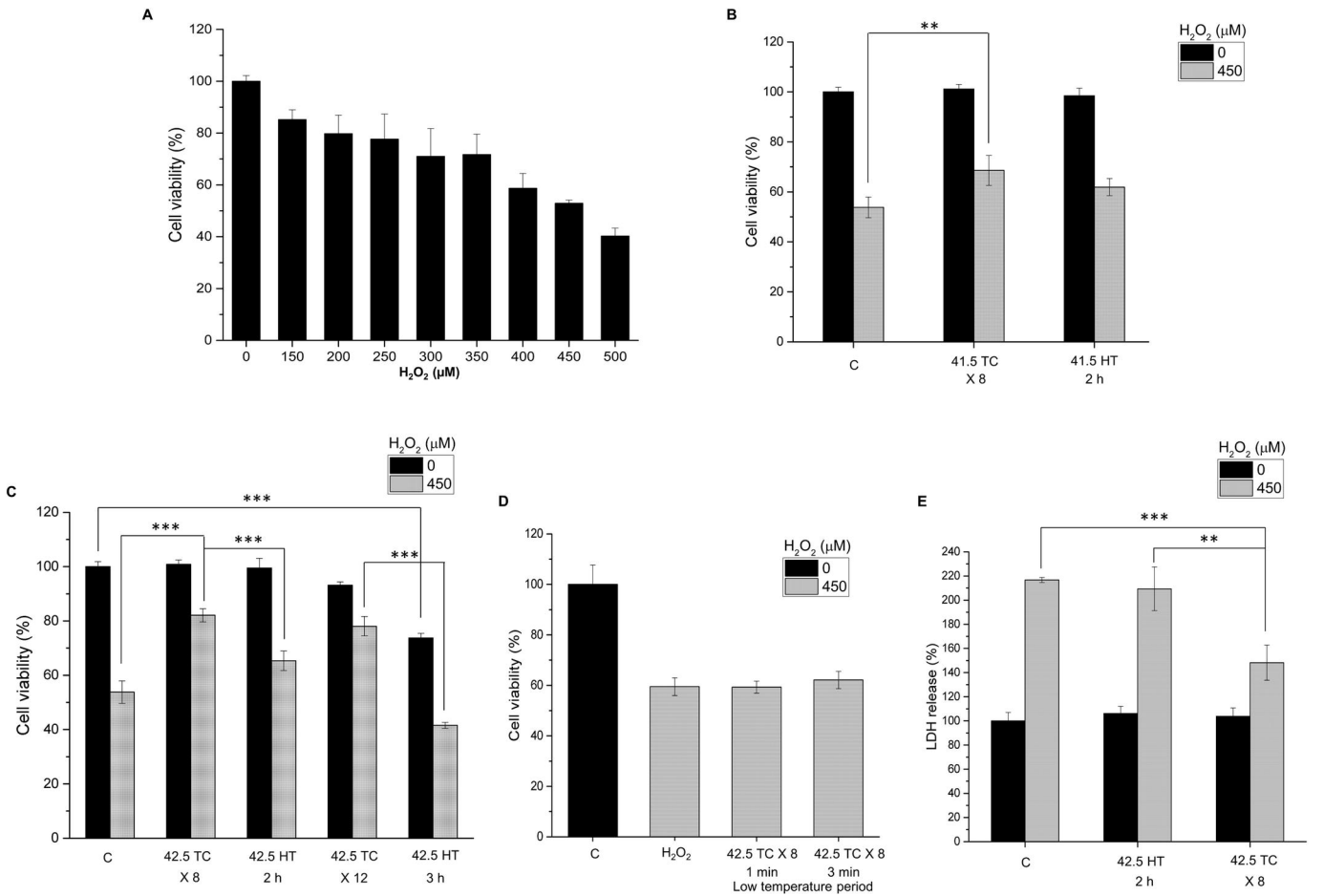
A
Cell viability (%)
120
100
80
60
40
20
0
0
150
200
250
300
350
400
450
500
H2O2 (μM)
B
**
H2O2 (μM)
0
450
Cell viability (%)
C
41.5 TC
X 8
41.5 HT
2 h
C
H2O2 (μM)
0
450
***
***
***
***
Cell viability (%)
C
42.5 TC
X 8
42.5 HT
2 h
42.5 TC
X 12
42.5 HT
3 h
D
H2O2 (μM)
0
450
Cell viability (%)
C
H2O2
42.5 TC X 8
1 min
42.5 TC X 8
3 min
Low temperature period
E
H2O2 (μM)
0
450
***
**
LDH release (%)
C
42.5 HT
2 h
42.5 TC
X 8

Figure 3

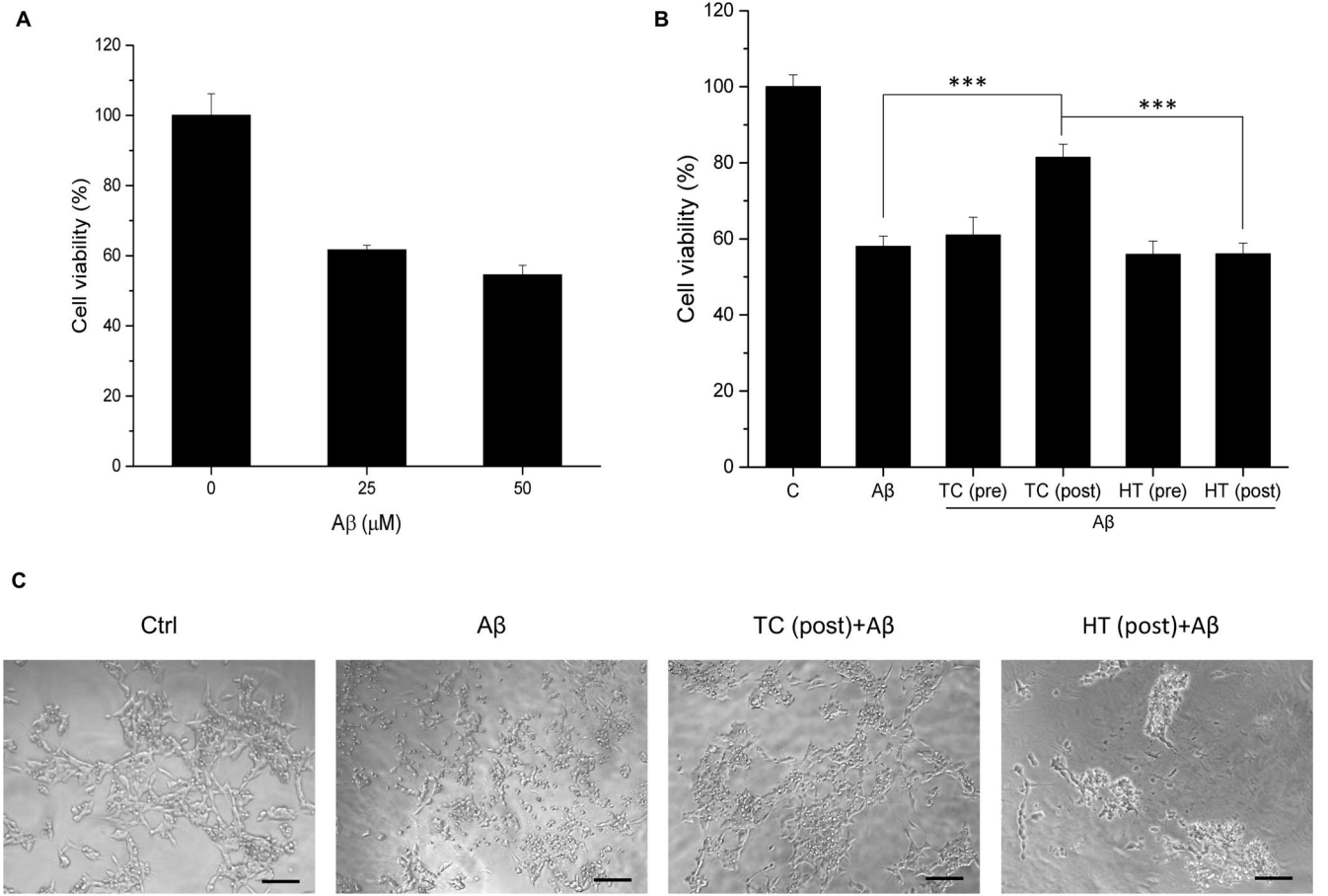
A
Cell viability (%)
120
100
80
60
40
20
0
0
25
50
Aβ (μM)
B
Cell viability (%)
120
100
80
60
40
20
0
***
***
C
Aβ
TC (pre)
TC (post)
HT (pre)
HT (post)
Aβ
C
Ctrl
Aβ
TC (post)+Aβ
HT (post)+Aβ

Figure 4

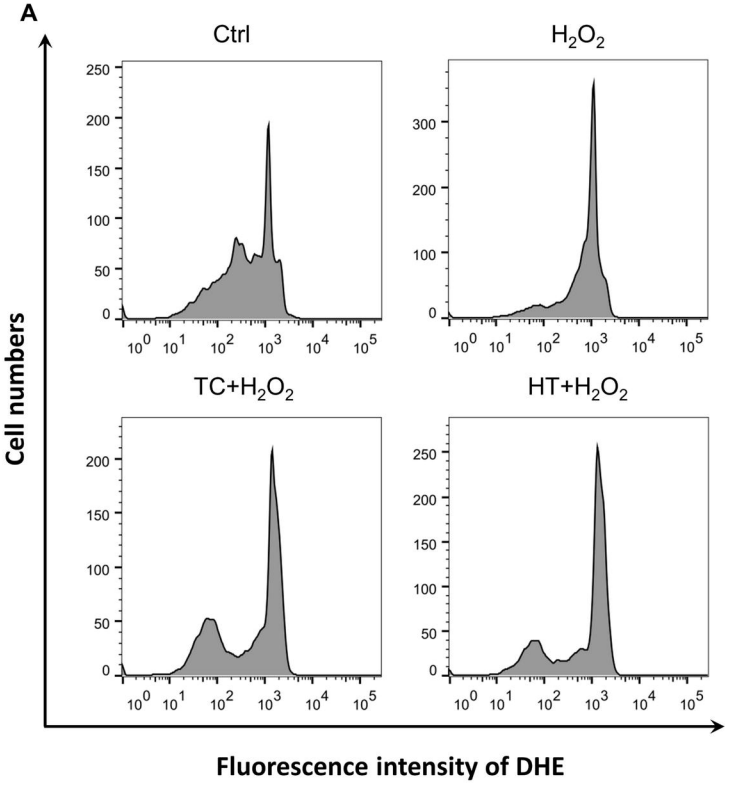
A
Ctrl
H2O2
TC+H2O2
HT+H2O2
Cell numbers
Fluorescence intensity of DHE

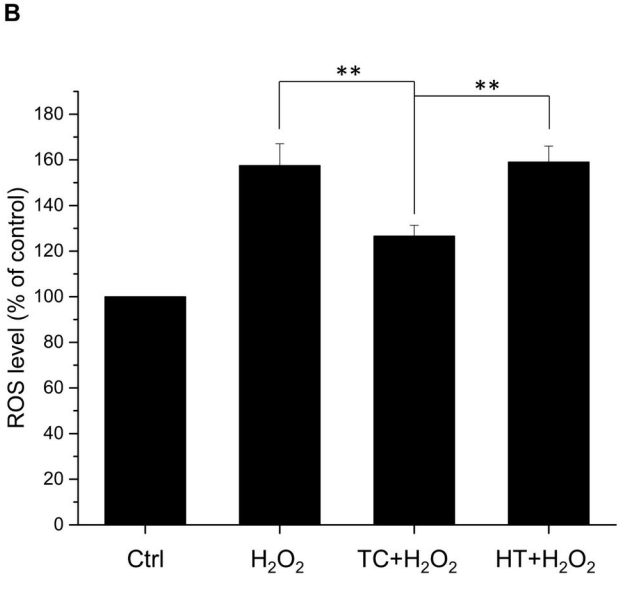
B
**
**
ROS level (% of control)
Ctrl
H2O2
TC+H2O2
HT+H2O2

Figure 5

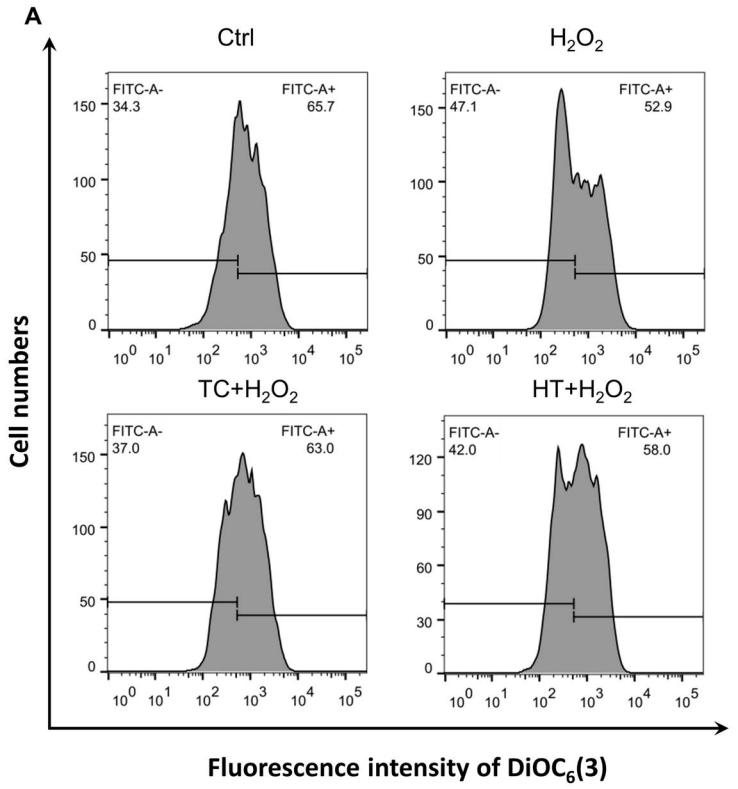
A
Ctrl
H_2O_2
TC+H_2O_2
HT+H_2O_2
FITC-A-
34.3
FITC-A+
65.7
FITC-A-
47.1
FITC-A+
52.9
FITC-A-
37.0
FITC-A+
63.0
FITC-A-
42.0
FITC-A+
58.0
Cell numbers
Fluorescence intensity of $DiOC_6(3)$

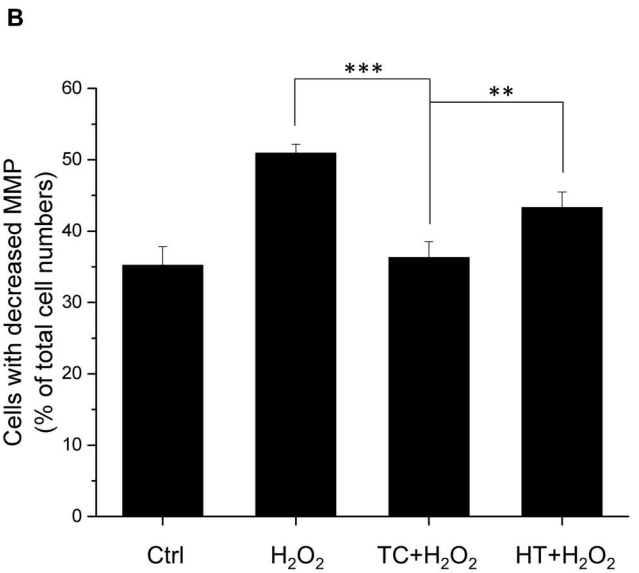
B
***
**
Cells with decreased MMP
(% of total cell numbers)
Ctrl
H_2O_2
TC+H_2O_2
HT+H_2O_2

Figure 6

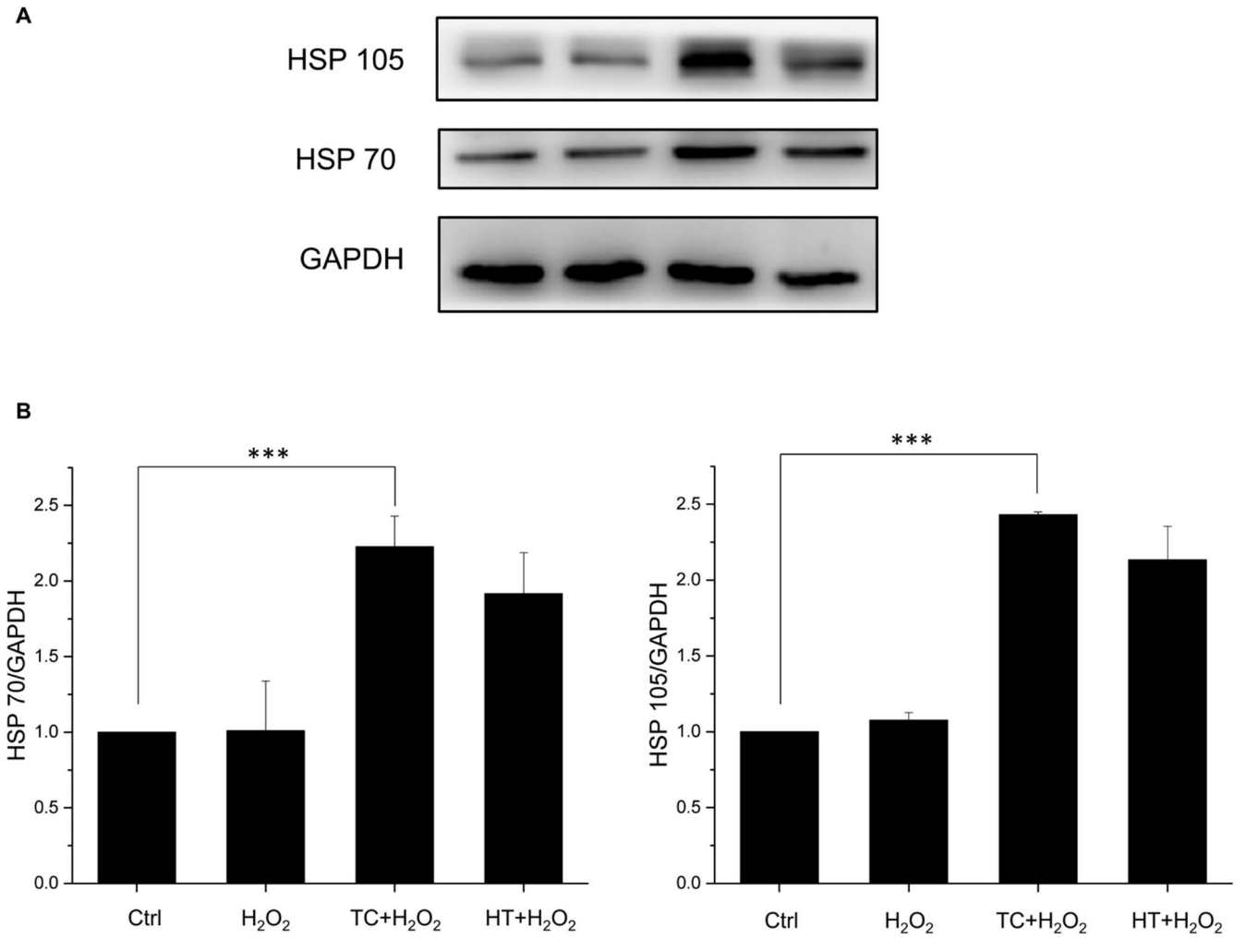
A
HSP 105
HSP 70
GAPDH
B
***
HSP 70/GAPDH
2.5
2.0
1.5
1.0
0.5
0.0
Ctrl
H2O2
TC+H2O2
HT+H2O2
***
HSP 105/GAPDH
2.5
2.0
1.5
1.0
0.5
0.0
Ctrl
H2O2
TC+H2O2
HT+H2O2

Figure 7

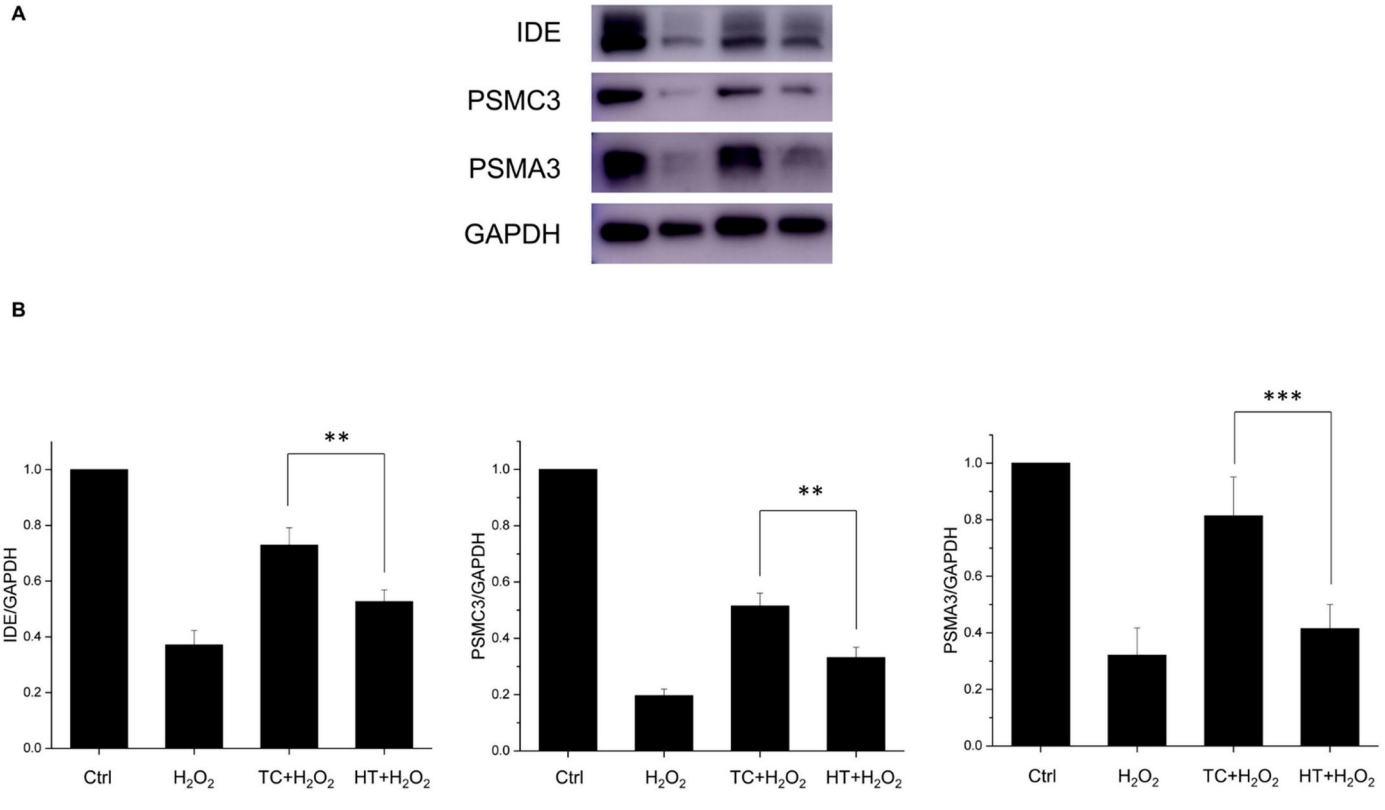
A
IDE
PSMC3
PSMA3
GAPDH
B
IDE/GAPDH
PSMC3/GAPDH
PSMA3/GAPDH
**
**
***
1.0
0.8
0.6
0.4
0.2
0.0
Ctrl
H2O2
TC+H2O2
HT+H2O2

Figure 8

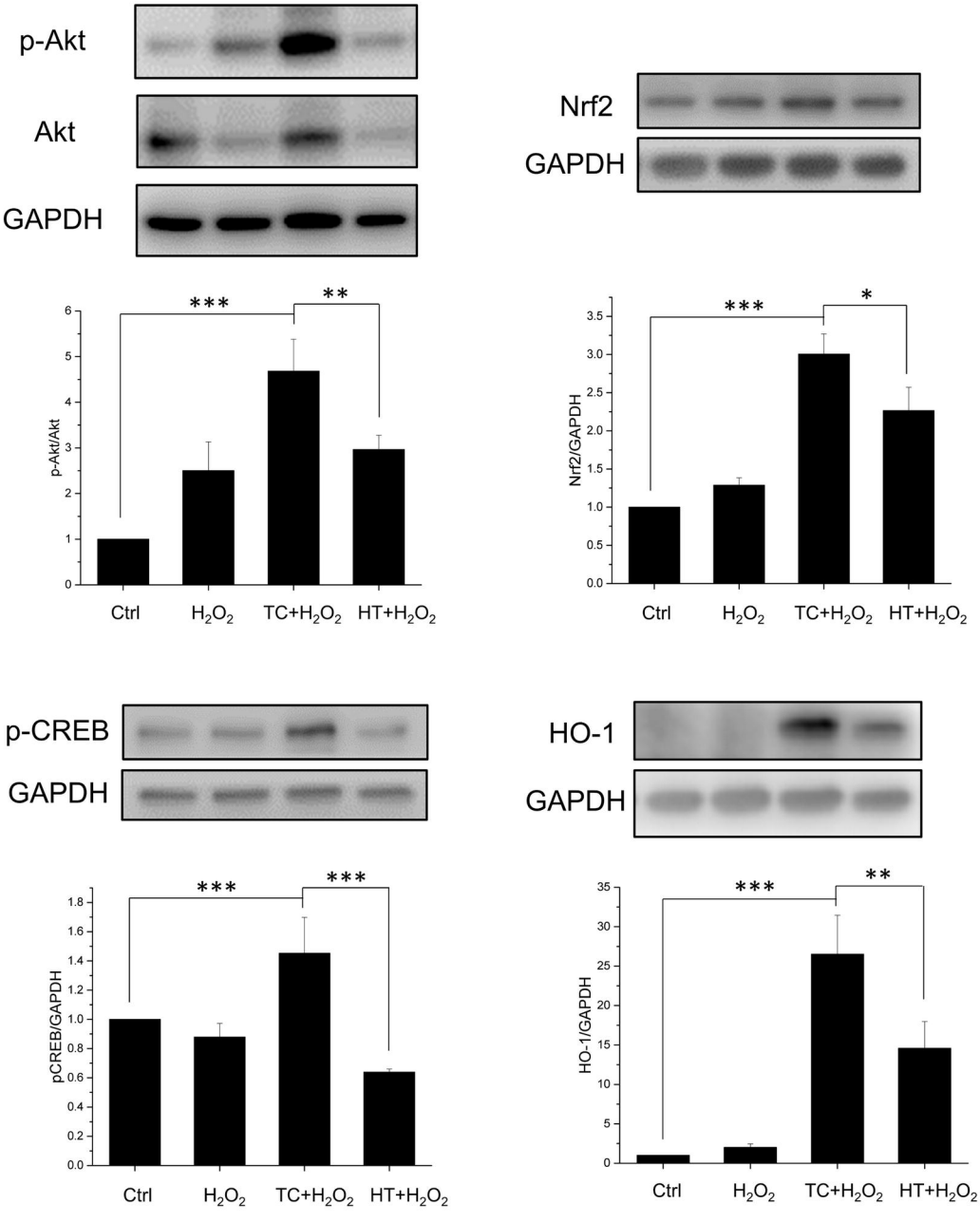
p-Akt
Akt
GAPDH
Nrf2
GAPDH
***
**
p-Akt/Akt
Ctrl
H2O2
TC+H2O2
HT+H2O2
***
*
Nrf2/GAPDH
p-CREB
GAPDH
HO-1
GAPDH
***
***
pCREB/GAPDH
***
**
HO-1/GAPDH

Figure 9

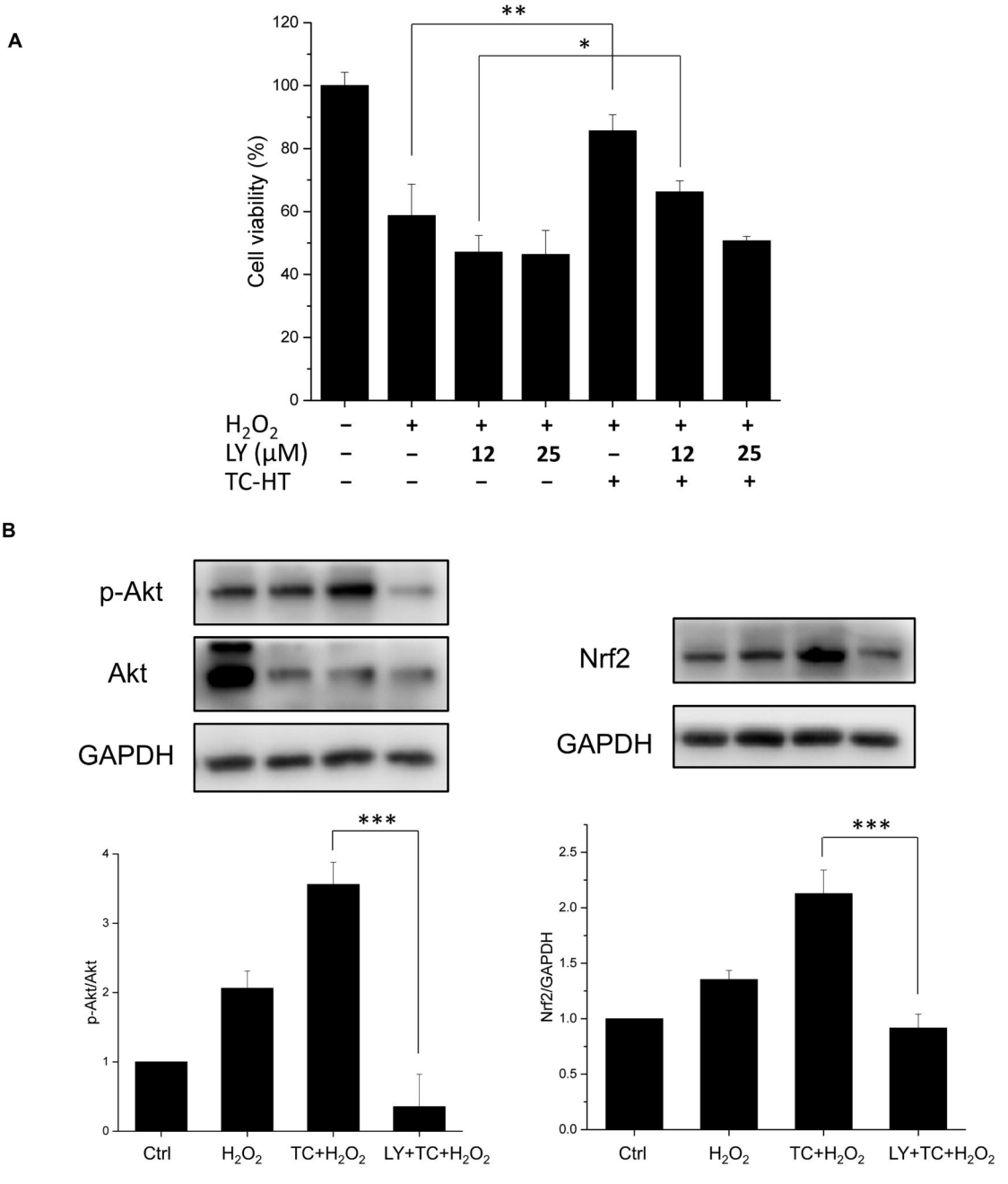
A
**
*
Cell viability (%)
120
100
80
60
40
20
0
H2O2 – + + + + + +
LY (μM) – – 12 25 – 12 25
TC-HT – – – – + + +
B
p-Akt
Akt
GAPDH
Nrf2
GAPDH
***
p-Akt/Akt
4
3
2
1
0
Ctrl
H2O2
TC+H2O2
LY+TC+H2O2
***
Nrf2/GAPDH
2.5
2.0
1.5
1.0
0.5
0.0
Ctrl
H2O2
TC+H2O2
LY+TC+H2O2

Figure 10

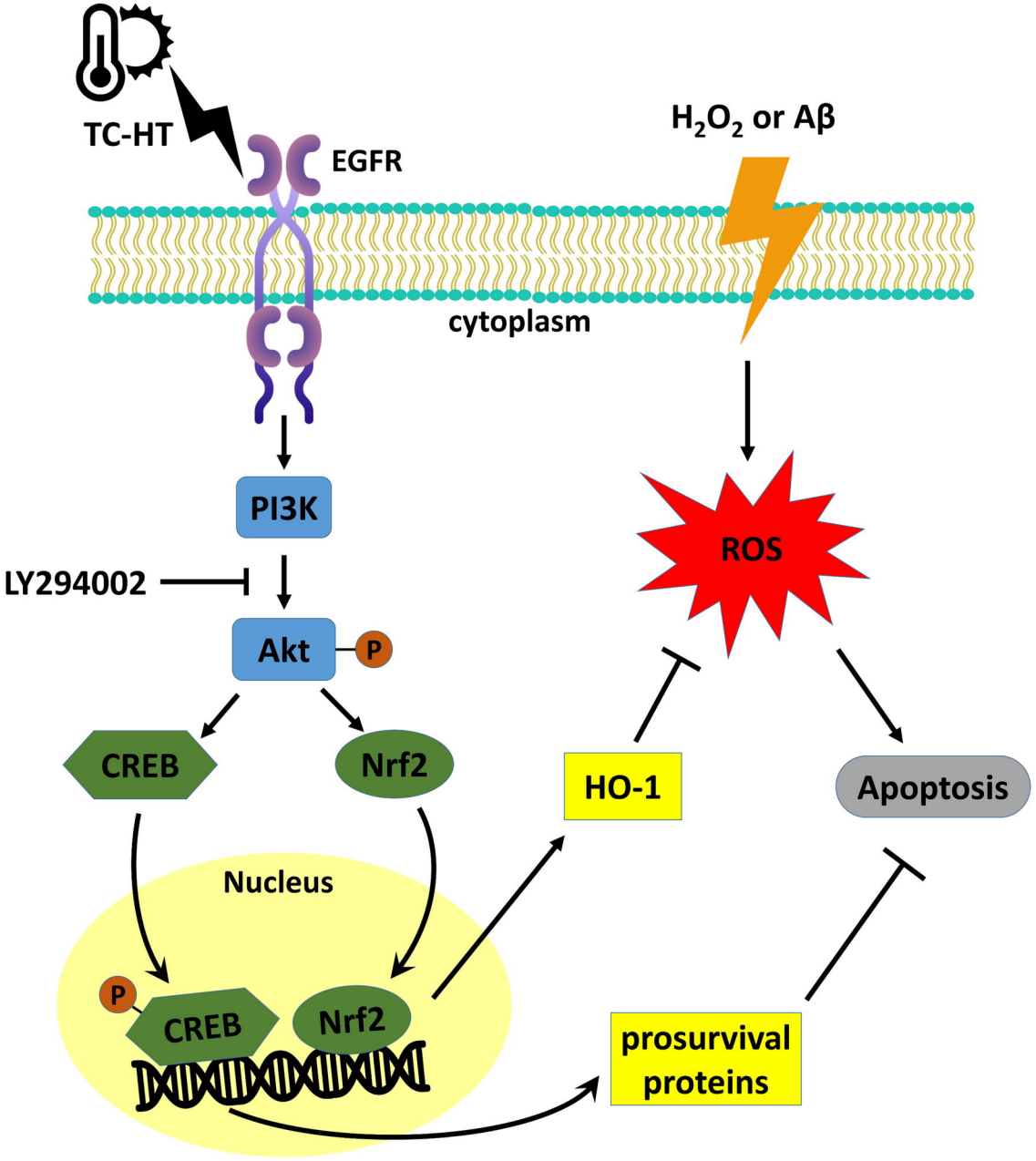
TC-HT
EGFR
H_2O_2 or Aβ
cytoplasm
PI3K
LY294002
Akt
P
ROS
CREB
Nrf2
HO-1
Apoptosis
Nucleus
P
CREB
Nrf2
prosurvival proteins